# Study of $^{200,202}$Po through $\beta^+$ and electron-capture decay and the manifestation of shape coexistence in the lighter Po isotopes

N. Bijnens, P. Decrock, S. Franchoo, M. Gaelens, M. Huyse, H.-Y. Hwang,* I. Reusen, J. Szerypo,†
J. von Schwarzenberg,‡ G. Vancraeynest, P. Van Duppen, and J. Wauters§
*Instituut voor Kern- en Stralingsfysica, University of Leuven, Celestijnenlaan 200 D, B-3001 Leuven, Belgium*

(Received 15 October 1998)

Levels in $^{200,202}$Po were studied via the $\beta^+$ and electron-capture decay of mass-separated At isotopes. Multiscaled singles $\gamma$, x, and conversion-electron spectra as well as $\gamma$-$\gamma$-t, $\gamma$-e$^-$-t, and x-e$^-$-t coincidences were measured. These isotopes contain key information for the presence of $\pi$(4p-2h) intruder configurations in the light Po isotopes. [S0556-2813(98)02008-1]

PACS number(s): 23.40.−s, 21.10.−k, 21.60.−n, 27.80.+w

## I. INTRODUCTION

Extensive studies on $0^+$ intruder states in even-even Pb, Hg, and Pt isotopes have been performed at several on-line mass-separators over the last ten years using $\beta^+$ and electron-capture and/or $\alpha$ decay (see, e.g., Ref. [1] and references therein). A large set of data on these low-lying $0^+$ excited states has now been established with, in some cases, deformed rotational-like bands built on top of them. The deformed configurations can be interpreted in terms of a proton-pair excitation across the closed $Z=82$ shell gap. These structures ''intrude'' into the low-energy structure due to a gain in total pairing energy and an increase in total proton-neutron interaction energy, which gives rise to two coexisting structures. Also in the odd-mass Tl ($Z=81$) and Bi ($Z=83$) isotopes intruder states have been observed at low energy and have been interpreted as $\pi(1p[1h_{9/2}]$-2h) and $\pi$(2p-1h$[3s_{1/2}]$) configurations, respectively [2–4]. A stringent test for the description of intruder states would be the identification of shape coexistence based on $\pi$(4p-2h) configurations above the $Z=82$ closed shell in the Po isotopes, corresponding to the excitation of two extra protons to the next major shell. Low-lying $0^+$ states have been observed in $^{198}$Po and $^{196}$Po fed by the $\alpha$ decay of $^{202}$Rn and $^{200}$Rn, respectively [5–7], and in $^{200,202}$Po populated by the $\beta$ decay of $^{200,202}$At [7]. Extra $2^+$ and $4^+$ states have been observed in $^{198,196}$Po by Alber *et al.* [8] and have been interpreted as belonging to a band built upon the $0^+$ excited states. This assignment has been questioned by Younes and Cizewski [9] who described the Po energy levels including the recently observed levels of $^{196-192}$Po [10–13] within the particle-core model (PCM) where the two protons are coupled to a vibrating core. To explain the microscopic evolution of collectivity, they calculated the quasiparticle-random-phase approximation (QRPA) wave functions of the $2_1^+$ states. Their results emphasize the critical role of the $\pi 1h_{9/2}$ and the $\nu 1i_{13/2}$ orbitals in the onset of collectivity in the polonium isotopes. Although the non-yrast $2^+$ and $4^+$ can be satisfactorily described (especially in $^{196,198}$Po) as predominantly multiphonon excitations, the model fails to reproduce the $0_2^+$ levels.

In this article, the detailed level schemes of $^{200,202}$Po which result from the $\beta$-decay studies of $^{200,202}$At are presented. It is advocated that these isotopes reveal the key information for the presence of intruder states in the low-energy level structures for $^{200}$Po and lighter Po isotopes.

## II. EXPERIMENTAL DETAILS

The $^{200,202}$At nuclei were produced in a fusion-evaporation reaction of 200 MeV $^{20}$Ne on $^{nat}$Re at the LISOL facility [14] in Louvain-La-Neuve. The beam energy was optimized for every product nucleus separately by using degrader foils. After extraction from the FEBIAD ion source [15] the reaction products were separated in Q/M in the analyzing magnet and implanted into an aluminized Mylar tape. The radioactivity was periodically moved from the implantation chamber to the decay position. For the detection of $\gamma$ rays, two high-purity germanium detectors were used, with respective efficiencies of 70% and 90% for the 1332.5 keV line of $^{60}$Co relative to the efficiency of an 3 inch×3 inch NaI(Tl) detector at a distance of 25 cm from the source. A low-energy germanium (LEGe) detector, with an active area of 1500 mm$^2$, was used to detect x rays and low-energy $\gamma$ rays. Standard $\gamma$-calibration sources were used for energy and intensity calibration of these detectors. A cooled Si(Li) detector (Schlumberger type with a thickness of 4 mm) was used to detect conversion electrons. A resolution (FWHM) of 2.1 keV was obtained for the 624-keV e$^-$ line of $^{137}$Cs. This e$^-$ detector was placed in the decay chamber at a distance of 4 cm from the Mylar tape. Energy and intensity calibrations of the electron detector were performed using transitions with known conversion coefficients. With this setup time-sequential $\gamma$-, x-, and electron-singles spectra were taken and $\gamma$-$\gamma$-t, $\gamma$-x-t, $\gamma$-e$^-$-t, and x-e$^-$-$\gamma$ coincidence events were collected.

*Present address: Mokwon University, 24 Mok Dong, Chung-Ku, Taejon, 301-729 Korea.

†Present address: Warsaw University, Institute of Experimental Physics, Hoza 69, 00681 Warsaw, Poland.

‡Present address: University of Notre Dame, Notre Dame, Indiana 46556.

§Present address: IMEC, Kapeldreef 75, B-3001 Leuven, Belgium.

 

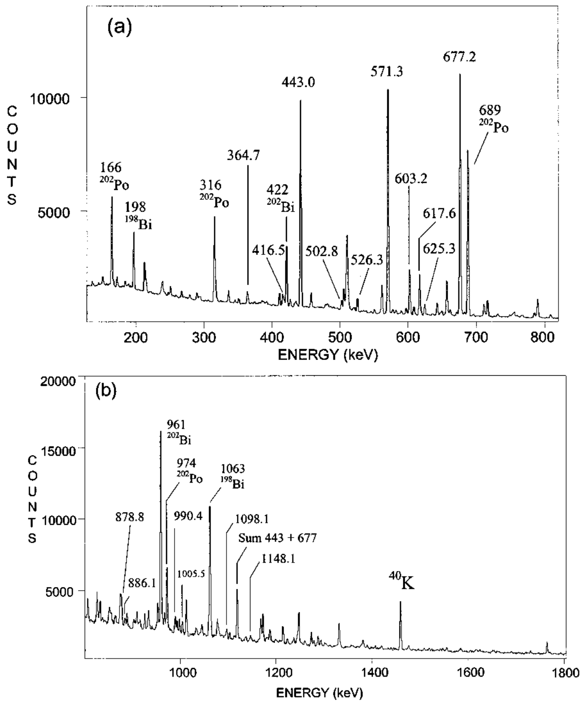


FIG. 1. The $\gamma$-ray spectrum obtained for $A=202$. Selected transitions have been indicated with their energy in keV. Those lines resulting from decay of a contaminant are labeled.

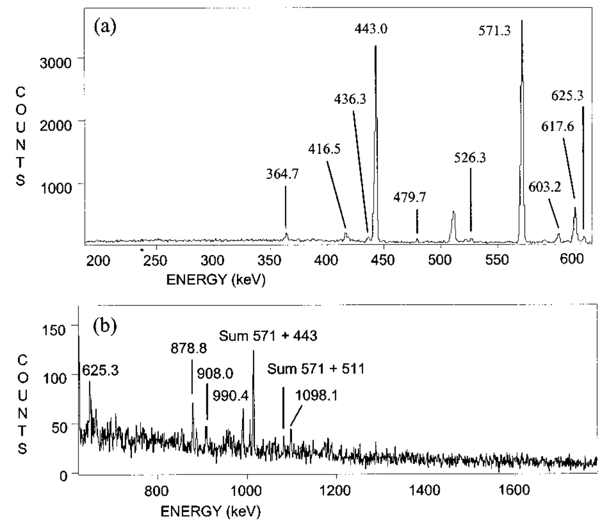


FIG. 2. The $\gamma$ spectrum obtained for $A=202$ in coincidence with the 666-keV $2^+ \rightarrow 0^+$ transition. The most intense lines are indicated with their energy (in keV).

### III. EXPERIMENTAL RESULTS

#### A. The $\beta^+$ and electron-capture decay of $^{202}$At

Previous to this paper, the most detailed information about the excited states of $^{202}$Po was available from in-beam studies of Beuscher *et al.* [16] and Fant *et al.* [17]. The study of the doubly-odd Fr-At-Bi $\alpha$-decay chains has yielded a rudimentary $\beta^+$ and electron-capture-decay scheme of $^{202}$At [18]. $\beta^+$ and electron-capture decay of $^{202}$Po was observed from two states; the $(7^+)$ isomer $[T_{1/2}=182(2)\text{ s}]$ as well as the $(2^+, 3^+)$ ground state $[T_{1/2}=184(1)\text{ s}]$. The heavy-ion fusion-evaporation reaction used in this study favors the high-spin isomer, but a non-negligible population of the low-spin ground state can be expected. From these results it is expected that the $\beta^+$ and electron-capture decay of $^{202}$At will feed low-spin levels as well as high-spin levels up to $I \approx 8\hbar$ in $^{202}$Po.

Figure 1 shows a $\gamma$-ray spectrum obtained for $A=202$. The transitions that are identified with the decay of $^{202}$At, on the basis of their half-life and x-e$^-$ or $\gamma$-$\gamma$ coincidence relations, are indicated with their energy in keV. The spectra are contaminated by $\beta$ decay from isobars and $\alpha$-decay daughter nuclei. The most intense lines contaminating the spectra are labeled. For the 677.2 keV $2^+ \rightarrow 0^+$ transition approximately $2.5 \times 10^5$ $\gamma$-ray counts have been collected in each Ge detector. A $\gamma$-ray spectrum that has been gated on this $2^+ \rightarrow 0^+$ transition with background subtraction is shown in Fig. 2. This results in a clean $^{202}$At $\beta$ and electron-capture-decay spectrum where all the lines from $\alpha$-decay daughter activity and the $^{202}$Po isobar are suppressed. True summing of the most intense $\gamma$ rays yields the most intense lines in the energy region $>1$ MeV. Figure 3 shows electron spectra obtained for $A=202$. The most intense electron transitions that belong to the decay of $^{202}$At are indicated with their transition energy. The energies and relative $\gamma$-ray intensities of all the transitions that belong to the decay of $^{202}$At are given in Table I together with their conversion coefficients and the multipolarity that has been deduced. A check was made if the corresponding e$^-$ lines were coincident with the characteristic Po-K x rays. A representative coincidence spectrum

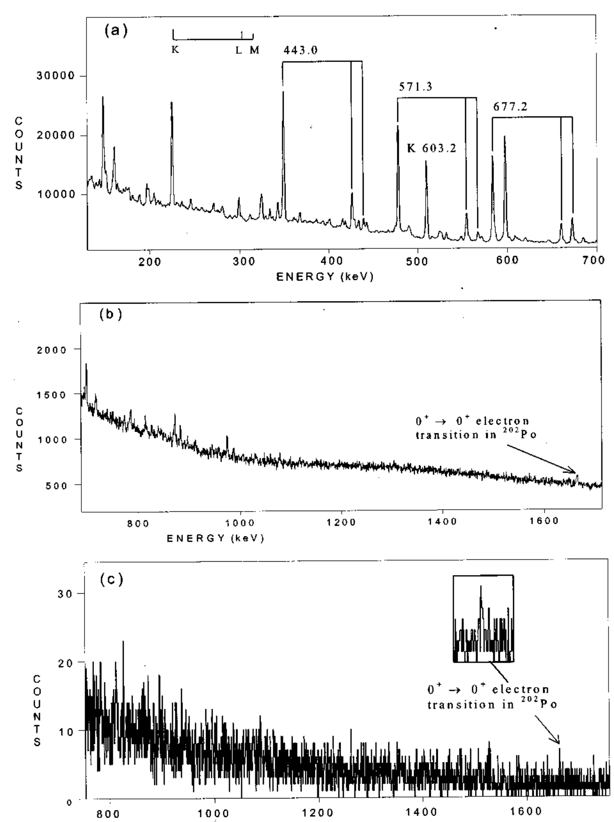


FIG. 3. The low energy (a) and high energy (b) e$^-$ spectra obtained for $A=202$. The electron transitions which belong to the decay of $^{202}$At are indicated with their transition energy (in keV). (c) shows an e$^-$ spectrum in coincidence with Po-K$_{\alpha 1}$ x rays.

TABLE I. The relative $\gamma$-ray intensities ($I_\gamma$) for transitions identified to the $\beta^+$ and electron-capture decay of $^{202}$At, conversion coefficients ($\alpha_K$ and $\alpha_L$), and multipolarity of transitions in $^{202}$Po. The theoretical conversion coefficients are taken from Rösel *et al.* [19]. ''Cal.'' indicates that the known multipolarity of these transitions has been used for the $e^- - \gamma$ intensity calibration.

| Energy (keV) | $I_\gamma$ | Experiment | Theory $E2$ | Theory $M1$ | Theory $E1$ | Multipolarity |
|---|---|---|---|---|---|---|
| 364.7(2) | 3.6(5) | K-0.036(5) | 0.044 | 0.26 | 0.017 | $E2$ |
| 387.0(5) | 1.8(5) | | | | | |
| 416.5(3) | 2.9(3) | K-0.09(2) | 0.033 | 0.18 | 0.012 | 61%$E2$/39%$M1$ |
| | | L-0.023(3) | 0.014 | 0.031 | 0.0021 | |
| 418.6(3) | 1.2(3) | K-0.12(4) | 0.033 | 0.178 | 0.012 | $M1$ |
| 436.3(2) | 1.8(6) | K-0.13(4) | 0.03 | 0.159 | 0.011 | $M1$ |
| 443.0(2) | 55(4) | K-cal. | 0.0288 | | | $E2$ |
| 479.7(4) | 1.4(4) | K-0.033(8) | 0.024 | 0.123 | 0.0092 | $E2$ |
| 502.8(2) | 2.6(7) | K-<0.012(4) | 0.022 | 0.11 | 0.0085 | ($E1$) |
| 525.8(5) | 1.4(5) | | | | | |
| 526.3(5) | 2.7(5) | | | | | |
| 536.0(3) | 0.5(3) | | | | | |
| 571.3(2) | 87(8) | K-cal. | 0.0172 | | | $E2$ |
| | | L-cal. | 0.00514 | | | |
| 591.0(2) | 0.8(4) | | | | | |
| 603.2(2) | 17.2(8) | K-0.057(4) | 0.016 | 0.068 | 0.0058 | $M1$ |
| 617.6(3) | 14.8(5) | K-0.0060(6) | 0.015 | 0.063 | 0.0056 | $E1$ |
| 619.0(3) | 1.2(5) | K-0.06(2) | 0.015 | 0.063 | 0.0055 | $M1$ |
| 625.3(2) | 3.6(5) | K-0.024(4) | 0.014 | 0.062 | 0.0054 | 79%$E2$/21%$M1$ |
| 677.2(2) | 100 | K-cal. | 0.0122 | | | $E2$ |
| | | L-cal. | 0.00314 | | | |
| 854.3(3) | 0.7(4) | | | | | |
| 878.8(3) | 2.1(5) | K-0.006(2) | 0.0075 | 0.026 | 0.0029 | $E2$ |
| 886.1(2) | 0.8(2) | K-0.009(3) | 0.0074 | 0.025 | 0.0028 | $E2$ |
| 908.0(5) | 0.7(2) | | | | | |
| 990.4(3) | 1.3(3) | K-0.006(2) | 0.0057 | 0.019 | 0.0023 | $E2$ |
| 1005.5(2) | 1.1(3) | K-0.005(2) | 0.0058 | 0.018 | 0.0022 | $E2$ |
| 1034.2(3) | 0.6(3) | | | | | |
| 1098.1(2) | 1.1(3) | | | | | |
| 1148.1(2) | 0.7(2) | | | | | |
| 1758(2) | | K->0.027 | 0.0021 | 0.0043 | | $E0$ |

is shown in Fig. 3(c). The tables of Rösel *et al.* [19] are used to determine the theoretical conversion coefficients. Due to the doublet structure and the low intensity of the 526-keV transition, we could not confirm the $E1$ multipolarity known from a previous measurement [17].

In Fig. 4 the level scheme of $^{202}$Po, developed from coincidence relations and the Ritz principle, is shown. The levels that were known from previous studies [17,18] and confirmed in our experiment are indicated with an asterisk. These are the yrast $2^+$, $4^+$, $6^+$, and $8^+$ states as well as the $5^-$ and $9^-$ states. The exact energy position of the $8^+$ isomer is not known because only some feeding transitions were observed. The $5^-$ level at 1866.6 keV has been suggested from decay studies [18], while the $9^-$ is known from in-beam work [17]. The additional energy levels will be discussed, concentrating first on the prompt coincidence transitions that feed the ground state, and then on the delayed coincidence transitions that feed the isomeric $8^+$ level at 1691.5+$\Delta$ keV [$T_{1/2}=85(15)$ ns [16,17]]. Some new weak lines that have been observed in this study, will be discussed at the end.

A first new level has been found at 1302.5 keV from the observation of a coincidence relation between the 677.2-keV $2^+\rightarrow 0^+$, the new 625.3-keV, and the 387.0-keV transition. The 625.3-keV transition was originally reported in Ref. [18]; but could not be placed. The coincidence relations observed here together with the intensity of the 625.3 and 387.0-keV transitions argue for a placement of the 625.3-keV transition on top of 677.2-keV level. The measurement of $\alpha_K=0.024$ (see Table I) is consistent with an assignment of 79%$E2$/21%$M1$ multipolarity for this transition. On the basis of this result and the systematics of the heavier Po isotopes, we assign $2^+$ for the spin and parity of this level at 1302.5 keV. No feeding to the ground state is observed down to the experimental limit of $I_\gamma<0.3\%$ relative to $I_\gamma(2_1^+\rightarrow 0_1^+)$.

A second $4^+$ level is observed at 1667.4 keV. This assignment is based on two new transitions: a 990-keV $E2$

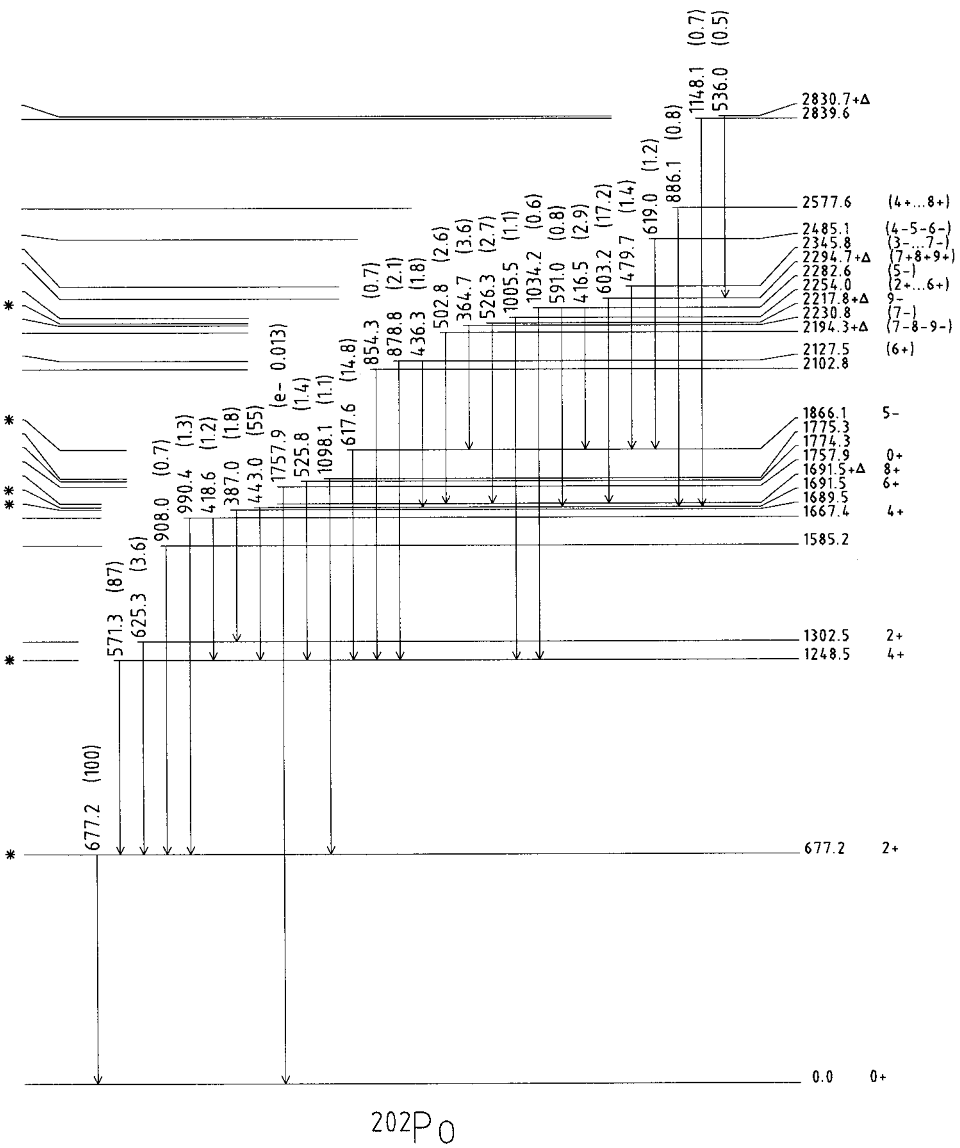


FIG. 4. The level scheme of $^{202}$Po, resulting from the $\beta^+$ and electron-capture decay of $^{202}$At. An asterisk is placed before the levels that are known from previous studies and are confirmed in our study.

transition coincident with the $2_1^+ \rightarrow 0_1^+$ transition and a 418.6-keV $M1$ transition which is coincident with the $4_1^+ \rightarrow 2_1^+$ transition as well as with the $2_1^+ \rightarrow 0_1^+$ transition. Feeding from this $4^+$ level at 1667.4 keV to the $2_2^+$ state at 1302.5 keV is not observed down to the experimental limit of $I_\gamma < 0.4\%$ relative to $I_\gamma(2_1^+ \rightarrow 0_1^+)$. The level at 1689.5 keV is based on the coincidence relation of the 387.0 keV $\gamma$ ray. This $\gamma$ ray shows only coincidences with the 625.3 and 677.2-keV transitions. Spin and parity for this level could not be deduced.

As discussed in Ref. [7], the position of a second $0^+$ state at 1758(2) keV is based on the observation of a fully converted transition to the ground state. This transition is coincident with Po-$K_{\alpha 1}$ x rays as can be seen from Fig. 3(c). From its half-life behavior, the absence of a corresponding $\gamma$-ray partner (resulting in a conversion coefficient much larger than for an $M1$ transition), and the absence of a coincidence relation with the $2_1^+ \rightarrow 0_1^+$ transition, we assign it as an $E0$ ground-state transition in $^{202}$Po. This electron transition has an intensity of $1.3(3) \times 10^{-4}$ relative to $I_\gamma(2_1^+ \rightarrow 0_1^+)$. We did not observe feeding from this $0_2^+$ state to the $2_1^+$ state down to the experimental limit of $I_\gamma < 0.5\%$ relative to $I_\gamma(2_1^+ \rightarrow 0_1^+)$.

The previously observed $5^-$ level at 1866.6 keV [18], based on a 617.8-keV transition populating the $4^+$ state, is confirmed in our measurement. The $\gamma$ ray originally observed at 617.8 keV [18] is in fact a doublet which can be separated as a 617.6-keV $E1$ transition $(5^- \rightarrow 4^+)$ and a 619.0-keV $M1$ transition. The 2127.5-keV level is assigned on the basis of an observed 878.8-keV $E2$ transition to the yrast $4^+$ state and a 436.3-keV $M1$ transition to the yrast $6^+$ state. A spin and parity assignment of $I^\pi = (6^+)$ for this level is preferred due to the similarity with $^{204}$Po [17]. A level at 2230.8 keV is based on the 364.7-keV $E2$ transition and its coincidence relations. The $E2$ multipolarity $[\alpha_K = 0.036(5)]$ together with the energy of this level provides support for a spin and parity assignment of $I^\pi = 7^-$, however, no $E1$ transition from this level to the $6^+$ level has been observed. This is in contrast with the Po isotopes of larger $N$, where a relatively strong $7^- \rightarrow 6^+$ is observed, but in the lighter isotopes ($^{198}$Po and $^{196}$Po) the $E2$ strength to the $5^-$ level is higher than the $E1$ strength to the $6_1^+$ level [10,20]. Therefore an assignment of $I^\pi = 7^-$ is not excluded. An excited state at 2282.6 keV is established from the observation of a 416.5-keV $E2/M1$ transition to the 1866.1-keV $5^-$ level. Transitions from this level have also been observed to the $6^+$ and $4^+$ states at 1691.5 and at 1248.5 keV, respectively. This decay pattern supports a spin and parity assignment of $I^\pi=(5^-)$ for this 2282.6-keV level.

Three transitions showed a delayed coincidence relation with the $6_1^+\rightarrow4_1^+\rightarrow2_1^+\rightarrow0_1^+$ cascade. From the TAC spectra a half life of ≈100 ns was determined. These transitions are placed feeding into the $8^+$ isomeric state which is known to have a half life of 85(15) ns [16,17]. No transitions could be placed feeding out of the $8^+$ level, thus the energy of this isomeric state could not be obtained in this study. The transition energy between the $8^+$ and $6^+$ states is indicated with a $\Delta$ symbol.

The 502.8-keV transition depopulates a level at $2194.3+\Delta$ keV which has been assigned $I^\pi=7^-$, $8^-$, or $9^-$ based on a conversion coefficient of $\alpha_{\mathrm{K}}<0.012(4)$ which indicates $E1$ multipolarity. The 526-keV $E1$ transition, although rather strong in in-beam measurements [17], is not intensely fed in our $\beta$-decay study. Furthermore, the 526-keV $\gamma$ ray consists of a fast and a delayed component with different coincidence relations and slightly different energies which complicates the analysis. Nevertheless, from the delayed component we can confirm the placement of a $9^-$ level at $2217.8+\Delta$ keV [16,17]. The most intense delayed line is the 603.2-keV transition, which was also observed in a previous measurement [18]. This $\gamma$ ray depopulates a level at $2294.7+\Delta$ keV which has been tentatively assigned $I^\pi=7^+, 8^+$, and $9^+$ based on a conversion coefficient of $\alpha_{\mathrm{K}}=0.057(4)$, indicating $M1$ multipolarity.

In this study, several weak $\gamma$ rays from the $\beta^+$ and electron-capture-decay of $^{202}$At have also been observed. The lines that are placed in the level scheme of $^{202}$Po are discussed in this paragraph. There is an indication for a level at 1585.2 keV out of the coincidence relation of the weak 908.0-keV $\gamma$ ray with the $2_1^+\rightarrow0_1^+$ transition. A level at 1774.3 keV is established from the fast component of the 526-keV transition. One third of the total intensity, corresponding to the low-energy part of this transition, for both $\gamma$ rays and $e^-$ lines, is coincident with the $4_1^+\rightarrow2_1^+\rightarrow0_1^+$ cascade but not with the 443.0-keV $6^+\rightarrow4^+$ transition. This indicates feeding into the yrast $4^+$ state and supports the placement of the 1774.3-keV level. The level at 1775.3 keV is based on a 1098.1-keV $\gamma$ ray and its coincidence relations. For both levels, no spin and parity could be deduced. There is an indication for a 2102.8-keV level via a 854.3-keV $\gamma$ ray and its coincidence relations. A level at 2254.0 keV is based on the observation of a coincident 1005.5-keV $\gamma$ ray with the $4^+\rightarrow2^+\rightarrow0^+$ cascade. It has been tentatively assigned $I^\pi=(2^+-6^+)$ based on the $E2$ multipolarity of the 1005.5-keV transition. A $I^\pi=(3^--7^-)$ state at 2345.8 keV is obtained from the coincidence relation of the 479.7-keV $E2$ transition with the $5^-\rightarrow4^+\rightarrow2^+\rightarrow0^+$ cascade. The 619.0-keV $M1$ transition from the doublet at 618 keV is coincident with the 617.6-keV transition indicating a level at 2485.1 keV with spin and parity $I^\pi=4^-$, $5^-$ or $6^-$. A 886.1-keV $E2$ transition is coincident with the $6_1^+\rightarrow4_1^+\rightarrow2_1^+\rightarrow0_1^+$ cascade and thus depopulates a $I^\pi=(4^+-8^+)$ state at 2577.6 keV. A level at 2839.6 keV has been obtained from the 1148.1-keV $\gamma$ ray which is coincident with the same cascade. A $\gamma$ ray of 536.0 keV shows a coincidence relation with the 603.2-keV $\gamma$ ray, indicating a level at $2830.7+\Delta$ keV.

### B. The $\beta^+$ and electron-capture decay of $^{200}$At

The level scheme for $^{200}$Po is similar to that observed for $^{202}$Po. It has been studied by in-beam gamma-ray spectroscopy by Maj *et al.* [20]. In addition, the study of the doubly odd Fr-At-Bi $\alpha$-decay chains has yielded a rudimentary $\beta^+$ and electron-capture-decay scheme of $^{200}$At [18]. Similar as in $^{202}$At it is mainly the $(7^+)$ isomer $[T_{1/2}=47(1)\ \mathrm{s}]$ at 104 keV in $^{200}$At from which $\beta^+$ and electron-capture decay occurs. The arguments given for $^{202}$At can be used for $^{200}$At and lead to a smaller $\beta^+$ and electron-capture decay intensity from the $(3^+)$ ground state $[T_{1/2}=43(1)\ \mathrm{s}]$. From these results, it is known that the $\beta^+$ and electron-capture decay of $^{200}$At feeds low-spin levels as well as high-spin levels up to $I\approx8\hbar$ in $^{200}$Po.

Figure 5 shows a $\gamma$-ray spectrum obtained for $A=200$. In a manner similar to Fig. 1, transitions from $^{200}$At as well as the most intense contamination lines are indicated with their energy in keV. For the 665.9-keV $2^+\rightarrow0^+$ transition more than $3\times10^5$ $\gamma$ rays have been collected in the two Ge detectors. A $\gamma$-ray spectrum which has been gated on this 665.9-keV $\gamma$ ray with subtraction of the background is shown in Fig. 6. This results in a clean $^{200}$At $\beta$ and electron-capture-decay spectrum where all the lines from $\alpha$-decay daughter activity and the $^{200}$Po isobar are suppressed. Due to the high efficiency of the germanium detectors, true-summing $\gamma$ rays from the most intense transitions have yielded the most intense lines in the energy region above 1 MeV. Figure 7 shows electron spectra obtained for $A=200$. The $e^-$ lines which belong to the decay of $^{200}$At are indicated with their transition energy. The coincidence relation between the $e^-$ lines and characteristic Po-K x rays was checked. A representative coincidence spectrum is shown in Fig. 7(c). The energies and the relative $\gamma$-ray intensities for the transitions that belong to the decay of $^{200}$At are given in Table II together with the conversion coefficients and the multipolarity that has been assigned for some transitions. Due to doublet structures in the singles spectra, the $E2$ multipolarity of the 323.8 keV $7^-\rightarrow5^-$ transition and the $E1$ multipolarity of the 373.8 keV $7^-\rightarrow6^+$ transition [20] could not be confirmed in our study. In Fig. 8 the level scheme of $^{200}$Po is shown. The levels, known from previous studies [18,20] that are confirmed in here are indicated with an asterisk. These are the yrast $2^+$, $4^+$, $6^+$, and $8^+$ states as well as the $5^-$, $7^-$, and $9^-$ negative parity states. All these states were known from in-beam work [20] and confirmed in decay studies [18]. We now discuss the additional energy levels, first by using the prompt coincidence relations and secondly by using delayed coincidence relations due to the feeding of the isomeric $8^+$ state at 1773.5 keV $[T_{1/2}=61(3)\ \mathrm{ns}\ [20]]$. New weak lines, that have been observed in this study, are discussed at the end of this section.

As mentioned in Ref. [7], the position of a second $0^+$ state at 1136.5 keV is based on the observation of a fully converted transition to the ground state. This transition is coincident with Po-$\mathrm{K}_{\alpha1}$ x rays as can be seen from Fig. 7(c). From its half-life behavior, the absence of a corresponding $\gamma$ ray (resulting in a conversion coefficient larger than for an $M1$ transition), and the absence of a coincidence relation with the $2_1^+\rightarrow0_1^+$ transition, it has been assigned as a $E0$ ground-state transition in $^{200}$Po. This 1043.4-keV K-$e^-$ line

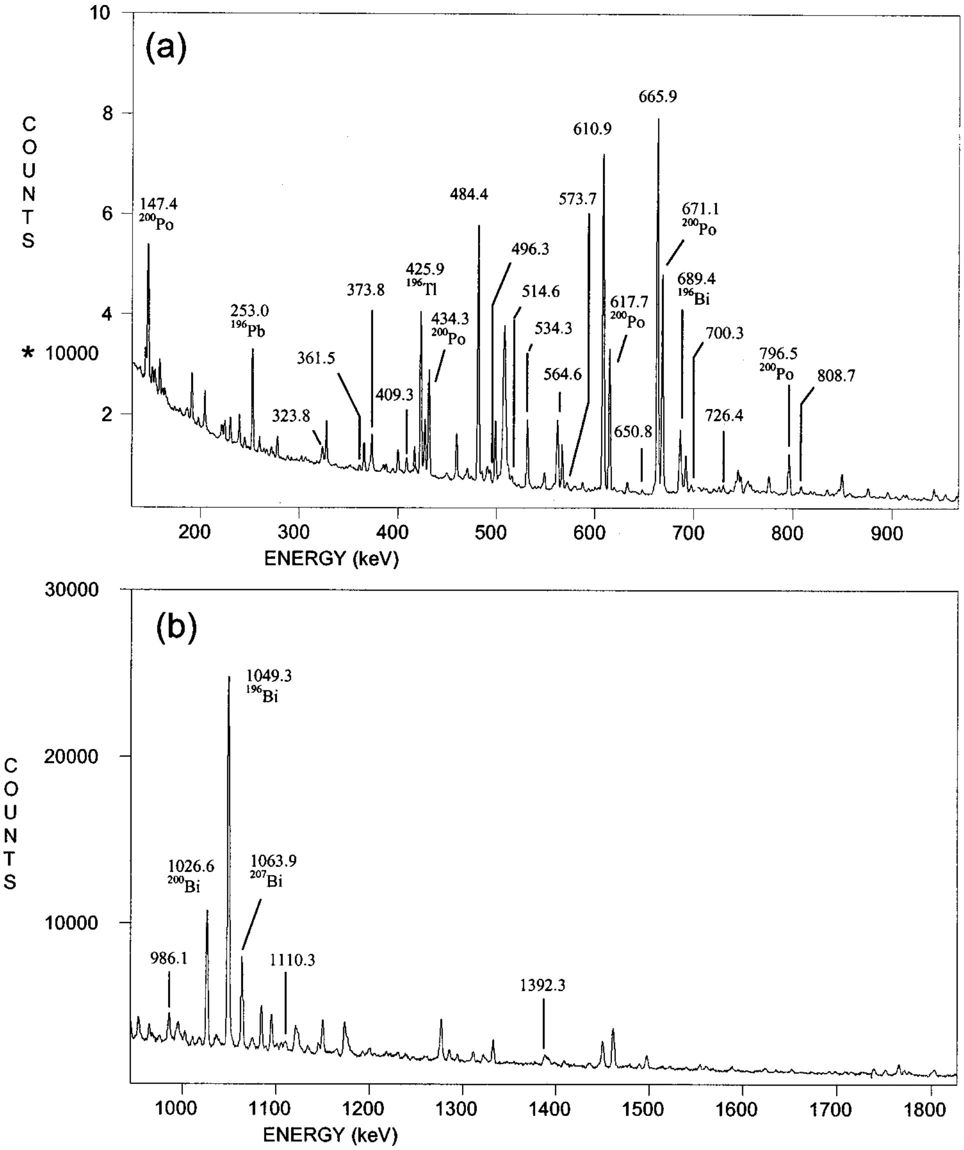


FIG. 5. The $\gamma$-ray spectrum obtained for $A=200$. Selected transitions have been indicated with their energy in keV. Those lines resulting from decay of a contaminant are labeled.

has an intensity of 4.5(10) $10^{-4}$ relative to $I_\gamma(2_1^+ \to 0_1^+)$. Feeding from this $0_2^+$ state to the $2_1^+$ state is not observed down to the experimental limit of $I_\gamma < 0.3\%$ relative to $I_\gamma(2_1^+ \to 0^+)$.

The level at 1392.3 keV is based on a $\gamma$ ray of 1392.3 keV which feeds the ground state and the 726.4-keV transition which has a coincidence relation with the $2_1^+ \to 0_1^+$ transition. Spin and parity, $2^+$, of this level are assigned by the strong $E0$ component in the conversion coefficient of the 726.4-keV transition. The corresponding 633-keV K-$e^-$ line is clearly coincident with the 665.9-keV $2_1^+ \to 0_1^+$ transition but not with the 610.9-keV $4_1^+ \to 2_1^+$ transition. The $2_2^+ \to 0_2^+$ transition is not observed down to the experimental limit of 0.2% for this transition relative to $I_\gamma(2_1^+ \to 0_1^+)$. The 1652.0-keV level is assigned on the basis of a 986.1-keV $\gamma$ ray that populates the yrast $2^+$ state. The 496.3-keV transition depopulates a level at 1773.1 keV that has been tentatively assigned $I=3^+$, $4^+$, or $5^+$ based on $\alpha_K = 0.11(4)$ which indicates $M1$ multipolarity. A level at 1791.4 keV is assigned on the basis of a 514.6-keV $\gamma$ ray that shows a coincidence relation with the $4_1^+ \to 2_1^+ \to 0_1^+$ cascade. This $\gamma$ ray has been reported in Ref. [18], but was not placed. The new 808.7-keV $\gamma$ ray also shows a coincidence relation with the $4_1^+ \to 2_1^+ \to 0_1^+$ cascade. The level at 2085.5 keV has been tentatively assigned $I^\pi = (2^+ - 6^+)$ based on a conversion coefficient of $\alpha_K = 0.009(2)$ that indicates $E2$ multipolarity for the 808.7-keV transition. The 409.3-keV $\gamma$ ray shows a coincidence relation with the $5^- \to 4_1^+ \to 2_1^+ \to 0_1^+$ cascade. The level at 2220.4 keV has been assigned $I=4^-$, $5^-$, and $6^-$ based on a conversion coefficient [$\alpha_K = 0.15(5)$] that indicates 74%$M1$/26%$E2$ multipolarity.

Two transitions showed a delayed coincidence relation with the $6^+ \to 4_1^+ \to 2_1^+ \to 0_1^+$ cascade. The population of the 361.5-keV $\gamma$ ray into the $8^+$ isomeric state at 1773.5 keV, which is known to have a half-life of 61(3) ns [20], has been confirmed. The 564.6-keV transition showed the same delayed behavior; from the TAC spectra a half-life of $\approx$70 ns was determined. The placement on top of the $8^+$ state is in contradiction with previous study [18] where the 564.6 keV was found to populate the $4_1^+$ state.

Similar to the 526-keV $E1$ transition in $^{202}$Po, the 488.0-keV $E1$ transition, although rather strong in in-beam measurements [20], is not intensively fed by the $\beta$-decay. We observed a weak coincidence relation with the $6_1^+ \to 4_1^+$ tran-

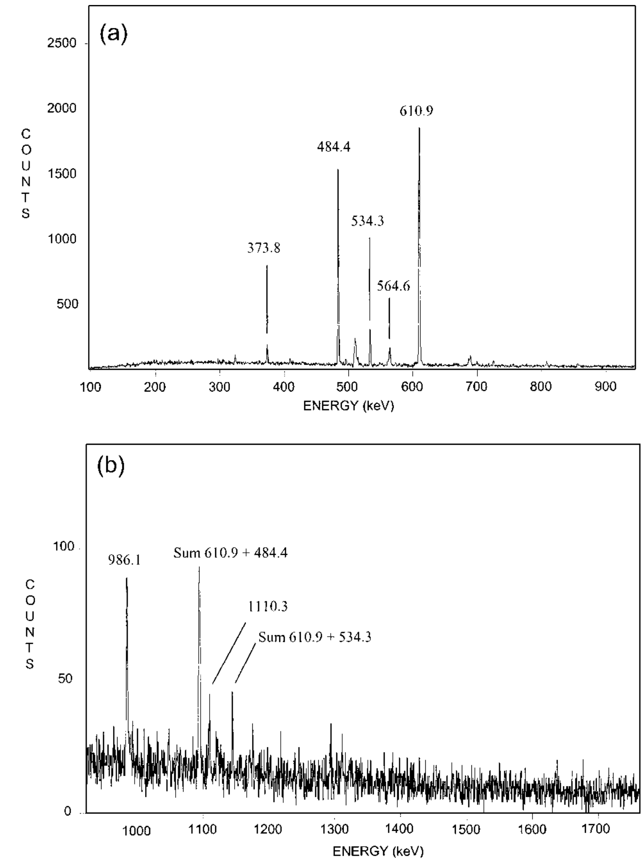


FIG. 6. The $\gamma$-ray spectrum obtained for $A=200$ in coincidence with the 666-keV $2^+\rightarrow 0^+$ transition. The most intense lines are indicated with their energy (in keV).

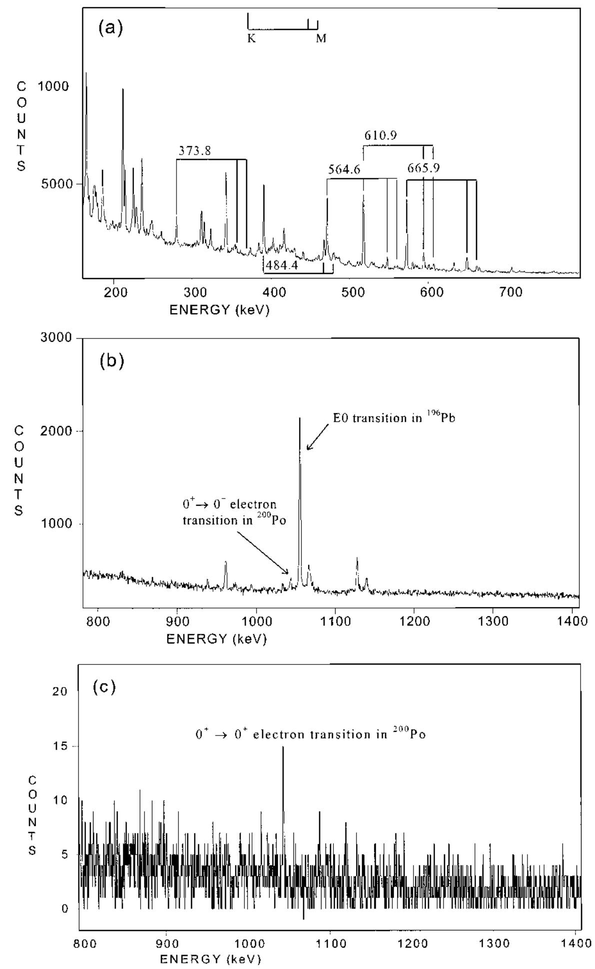


FIG. 7. The low energy (a) and high energy (b) $e^-$ spectra obtained for $A=200$. The electron transitions belonging to the decay of $^{200}$At are indicated by their transition energy (in keV). (c) shows an $e^-$ spectrum in coincidence with Po-$K_{\alpha 1}$ x rays.

sition and coincidence relations with the $4^+\rightarrow 2_1^+$ and $2_1^+\rightarrow 0_1^+$ transitions. Based on these observations the $9^-$ level at 2261.5 keV is confirmed [20].

Some weak $\gamma$ rays which have been observed, are discussed below. The 1110.3-keV $\gamma$ ray and its coincidence relation with the $2_1^+\rightarrow 0_1^+$ transition support the placement of a level at 1776.2 keV. Two weak $\gamma$ rays show a coincidence relation with the $4_1^+\rightarrow 2_1^+\rightarrow 0_1^+$ cascade: the 573.7-keV $\gamma$ ray depopulating a level at 1850.5 keV, and the 606.3-keV $\gamma$ ray depopulating a level at 1883.1 keV. This level at 1883.1 keV has been tentatively assigned $I=3^+$, $4^+$, or $5^+$ based on the $M1$ multipolarity of the 606.3-keV transition. It should be noted here that our final analysis (taking all the data from all detectors into account) resulted in a larger $\gamma$ intensity for this 606.3-keV transition, leading to the current conversion coefficient [$\alpha_K=0.6(2)$] which is lower than previous published value [7] [$\alpha_K=0.94(12)$]. We attribute a $M1$ character to this transition where the previous value assumed $E0/M1/E2$.

The 603.2-keV and 650.8-keV $\gamma$ rays have been observed in coincidence with the $5^-\rightarrow 4_1^+\rightarrow 2_1^+\rightarrow 0_1^+$ cascade. The 603.2-keV $E0/M1/E2$ transition argues for another $(5^-)$ state at 2414.3 keV. The 2461.9-keV level has been assigned $I^\pi=4^-$, $5^-$, or $6^-$ based on the $M1/E2$ multipolarity of the 650.8-keV transition. The level at 2461.5 keV is based on the 700.3-keV $M1$ transition and its coincidence relation with the $6^+\rightarrow 4^+\rightarrow 2^+\rightarrow 0^+$ cascade.

## IV. DISCUSSION

Figure 9 shows the positive ($I=2^+-8^+$) and negative parity yrast states ($I=5^- - 11^-$) as well as the nonyrast $0_2^+$, $2_2^+$, and $4_2^+$ states for the even-even isotopes from $^{192}$Po to $^{210}$Po. First, a review on the present understanding of the structure of the negative and positive parity states will be given followed by a discussion of the properties of specific levels in $^{202,200}$Po. The two isotopes in this study, $^{202,200}$Po, cover a transition region between the heavier isotopes $N>118$ which can be satisfactorily described, and the lighter isotopes which show a more complex behavior. We will show that the $^{202,200}$Po isotopes contain key information necessary to understand the properties of the lighter isotopes.

### A. Negative parity states

Due to their striking similarity with the Pb isotopes, the $5^-$, $7^-$, and $9^-$ states up to $^{198}$Po have been classified as neutron states [20]. The two-neutron configurations involve a $\nu(1i_{13/2})$ hole coupled to a $p_{1/2}$, $p_{3/2}$, or $f_{7/2}$ neutron hole. The energy of the $(7^-)$ level in $^{202}$Po that has been found in this study is very consistent with the $7^-$ levels observed in other Po nuclei. The systematic trend in these levels is very

TABLE II. Relative $\gamma$-ray intensities ($I_\gamma$) for transitions identified to the decay of $^{200}$At, conversion coefficients ($\alpha_K$ and $\alpha_L$), and multipolarity of transitions in $^{200}$Po. The theoretical conversion coefficients are taken from Rösel *et al.* [19]. ''Cal.'' indicates that the known multipolarity of these transitions has been used for the $e^- - \gamma$ intensity calibration.

| Energy (keV) | $I_\gamma$ | Experiment | Theory $E2$ | $M1$ | $E1$ | Multipolarity |
|---|---|---|---|---|---|---|
| 323.8(2) | 2.4(6) | K-0.23(6) | 0.057 | 0.36 | | $(E2)^a$ |
| | | L-0.047(13) | 0.0026 | 0.061 | | |
| 361.5(2) | 0.7(2) | | | | | |
| 373.8(2) | 7.1(7) | K-<0.09 | 0.042 | 0.24 | 0.016 | $(E1)^a$ |
| 409.3(2) | 2.5(4) | K-0.15(5) | 0.034 | 0.19 | 0.013 | 74%$M1$/26%$E2$ |
| 484.4(2) | 48(4) | K-cal. | 0.0239 | | | $E2$ |
| | | L-cal. | 0.00838 | | | |
| 488.4(2) | 1.8(6) | | | | | |
| 496.3(2) | 2.2(6) | K-0.11(4) | 0.023 | 0.11 | 0.0086 | $M1$ |
| | | L$^b$ | | | | |
| 514.6(2) | 4.5(6) | | | | | |
| 518.5(3) | 1.5(4) | | | | | |
| 534.3(2) | 16(3) | K-0.0075(14) | 0.021 | 0.091 | 0.0081 | $E1$ |
| 549.3(2) | 0.7(3) | | | | | |
| 564.6(2) | 13(3) | K-0.09(2) | 0.018 | 0.081 | 0.0066 | $M1$ |
| | | L-0.014(3) | 0.005 | 0.014 | 0.0011 | |
| 573.7(2) | 0.9(3) | | | | | |
| 603.2(2) | 0.6(2) | K-0.15(4) | 0.015 | 0.068 | 0.0058 | $E0/M1/E2$ |
| | | L-0.08(3) | 0.0043 | 0.012 | 0.00094 | |
| 606.3(4) | 1.1(4) | K-0.06(2) | 0.015 | 0.067 | 0.0058 | $M1$ |
| 610.9(2) | 84(8) | K$^b$ | | | | $E2$ |
| | | L-cal. | 0.00418 | | | |
| 650.8(2) | 1.2(2) | K-0.033(7) | 0.013 | 0.056 | 0.0050 | 53%$E2$/47%$M1$ |
| 665.9(2) | 100 | K-cal. | 0.0126 | | | $E2$ |
| | | L-cal. | 0.00329 | | | |
| 700.3(3) | 1.0(6) | K-0.09(5) | 0.011 | 0.046 | 0.0044 | $M1$ |
| 726.4(6) | 1.4(2) | K-0.11(3) | 0.011 | 0.042 | 0.0041 | $E0/M1/E2$ |
| 808.7(7) | 2.9(4) | K-0.009(2) | 0.0088 | 0.031 | 0.0033 | $E2$ |
| 986.1(2) | 3.0(6) | K-0.011(3) | 0.0068 | 0.019 | 0.0023 | 66%$E2$/34%$M1$ |
| 1110.3(2) | 1.1(3) | | | | | |
| 1136.5(6) | | K->0.08 | 0.0046 | 0.013 | 0.0018 | $E0$ |
| 1392.3(3) | 1.2(4) | | | | | |

[a]The multipolarity in brackets from a previous study [20] could not be confirmed due to doublet structures.
[b]No values have been deduced due to doublet structures.

similar to these states observed in Pb isotopes. It should be noted, however, that in $^{196}$Po the similarity with the $^{194}$Pb isotone (see Fig. 10 in Ref. [20]) is less pronounced.

As can be seen from Fig. 9, the $11^-$ level, identified as a $\pi h_{9/2}\ \pi i_{13/2}$ configuration [23], shows a rather constant behavior. However a remarkable increase has been observed in the $B(E3;\ 11^- \rightarrow 8^+)$ values from a few W.u. for $^{202}$Po to 27(5) W.u. in $^{196}$Po [8,20]. It has been suggested in Ref. [8] that this is due to small $(3^-)\otimes(8^+)$ admixtures in the $11^-$ state.

### B. The yrast $2^+$, $4^+$, $6^+$, and $8^+$ states

The $^{210}$Po ($N=82$) levels up to $\approx$3 MeV have been described using a modified surface delta interaction (MSDI) within the proton ($1h_{9/2}, 2f_{7/2}, 1i_{13/2}$) model space [24]. For the yrast $2^+-4^+-6^+-8^+$ states, the $\pi(1h_{9/2})^2$ configuration is dominant, giving rise to the well known shell-model broken-pair structure. In $^{208}$Po the opening of the neutron shell results in $2^+$, and to a lesser extent also $4^+$ levels decreasing in energy. For the $2^+$ state this drop in energy has been described as a structure change from the proton configuration to a rather pure neutron-hole configuration [25].

Down to $^{200}$Po the energy of the $2^+$ yrast state stays rather constant while the $4^+$, $6^+$, and $8^+$ states show a smooth increase in energy for reducing neutron number. From g-factor measurements of the $8^+$ isomer and $B(E2;\ 8^+ \rightarrow 6^+)$ values, it has been suggested that the wave functions of the $8^+$ and $6^+$ levels remain reasonably pure two-proton configurations up to $^{200}$Po [20], while the energy of the $2^+$ and $4^+$ states deviates from a pure $\pi(1h_{9/2})^2$ level structure. Recently Younes and Cizewski [9] showed that this deviating energy can be explained by coupling of the

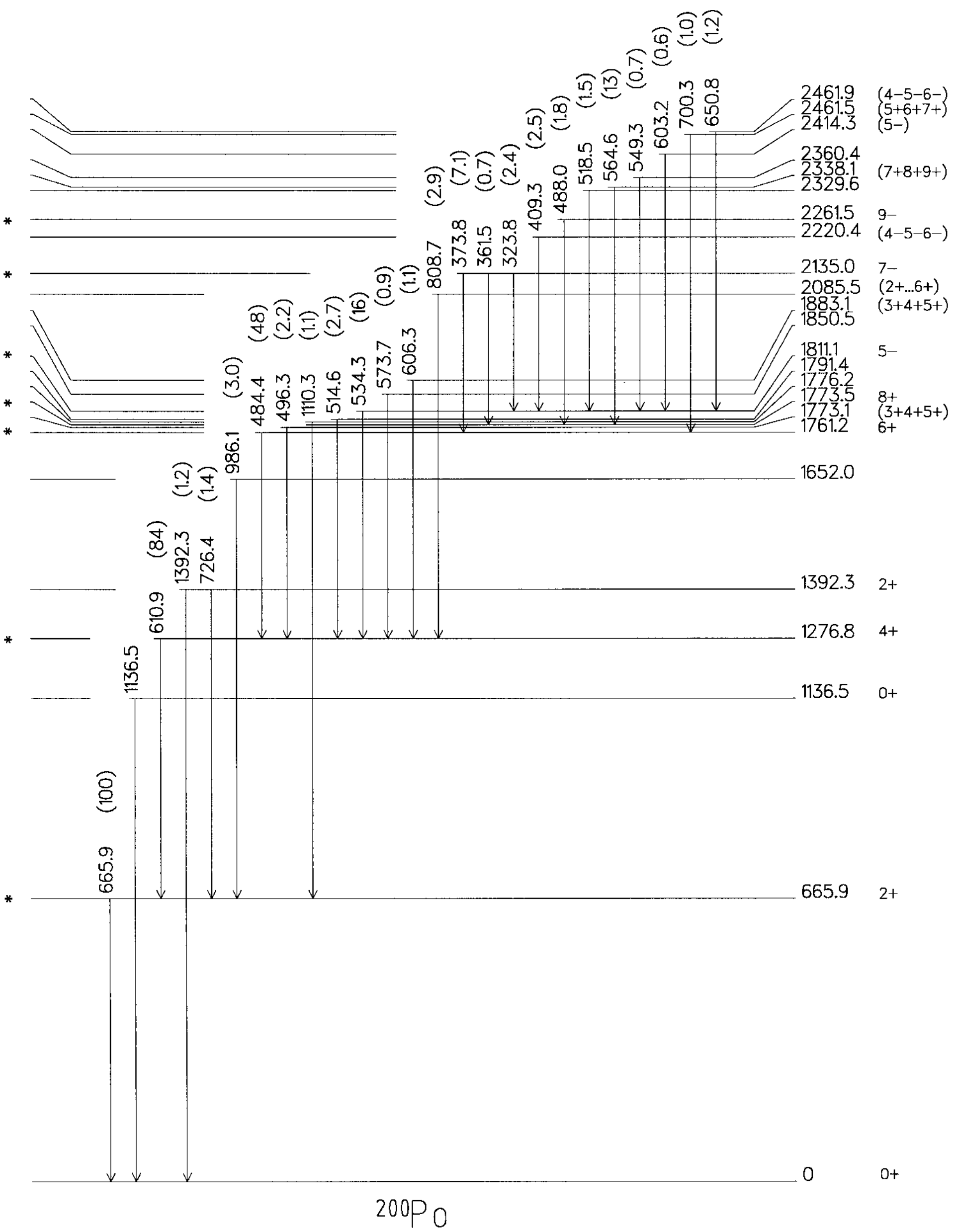


FIG. 8. The level scheme of $^{200}$Po which results from the $\beta^+$ and electron-capture decay of $^{200}$At. An asterisk indicates that the level was known from previous studies and is confirmed in our study.

two outer protons to a vibrating core. Within this particle-core model, the energy of the $2^+$, $4^+$, $6^+$, and $8^+$ states down to $^{200}$Po were reproduced [9]. In this framework, the $2^+$ and $4^+$ levels are explained as pure 1 and 2 phonon states respectively, while the $6^+$ and $8^+$ states are interpreted as pure zero-phonon excitations [i.e., $\pi(1h_{9/2})^2$].

The nucleus, $^{200}$Po, seems to be the transition point in this smooth trend of the properties of the heavier isotopes. From $^{200}$Po on the $6^+$ and $8^+$ states separate from each other. The $B(E2;8^+\rightarrow 6^+)$ value drops from 9.4(5) W.u. in $^{200}$Po down to 2.0(1) W.u. in $^{198}$Po which is suggested to result from a configuration change in the $6^+$ state [20]. Furthermore the $2^+$ and $4^+$ levels also smoothly decrease in energy. Until now this gradual change of the low-energy level structure for $A\leqslant 198$ has been interpreted in two different ways. A first description is based on mixing between the normal states and the intruding deformed band [7,26]. A second interpretation has been given within the PCM model [9]. Younes and Cizewski showed that the decreasing trends of the $2^+$, $4^+$, and

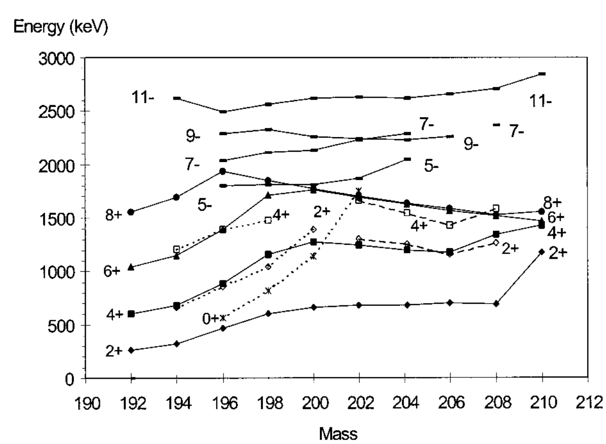


FIG. 9. The positive ($I^\pi=2^+-8^+$) and negative yrast parity states ($I^\pi=5^- - 11^-$) as well as the nonyrast $0_2^+$, $2_2^+$, and $4_2^+$ states for the even-even isotopes from $^{192}$Po to $^{210}$Po. Data have been taken from Ref. [9,12,21,22] and present work.

$6^+$ levels are reproduced only by including a sharp rise of the proton-core interaction parameter. The PCM phonon wave functions become increasingly mixed when going to the lighter Po isotopes. This has been interpreted as a change in the intrinsic structure of the phonon core. To get more insight into the microscopic nature of the vibration, QRPA calculations have been carried out to extract semimicroscopic wave functions for the $2^+$ states, which have been interpreted as the analogs of the phonons in the PCM calculations. From this comparison a link was established between the $\nu 1i_{13/2}$ orbital which becomes dominant in the neutron component of the $2^+$ wave function and an increase of collectivity in the lighter Po isotopes. The PCM phonon wave functions give a good description for the $A>200$ Po isotopes, however, for $^{200}$Po and lighter isotopes the model fails to reproduce some experimental states, in particular, the $0_2^+$ states.

### C. The $0_2^+$, $2_2^+$, and $4_2^+$ states

For almost all currently observed Po isotopes with $A \leqslant 208$, second $2^+$ and $4^+$ states have been identified. In $^{198,196}$Po, these states have been interpreted as members of a $\pi$(4p-2h) deformed oblate band with a $[(\pi s_{1/2})^{-2}(\pi h_{9/2})^4]$ configuration [8]. However, it should be noted that the $2_2^+$ and $4_2^+$ states are always close in energy to the $4_1^+$ and $6_1^+$ states respectively, which, within the PCM model, can be ascribed to the predominantly multiphonon character of these states [9]. The $0_2^+$ states, however, are not consistent with the latter description, as they should be nearly degenerate with the $4_1^+$ and $2_2^+$ states. In a previous paper [7], these $0_2^+$ states were interpreted as $\pi$(4p-2h) deformed intruder configurations. The $2_2^+$ states in $^{196,200}$Po and the $4_2^+$ states in $^{196,198}$Po were interpreted as the first members of a collective band built on top of these $0_2^+$ intruder states. The main argument used was the characteristic lowering of the excitation energy of the $0_2^+$, $2_2^+$, and $4_2^+$ states when reducing the neutron number towards midshell between $N=82$ and 126 similar as in the Pb, Hg, and Pt isotopes [1]. In order to resolve the disagreement between the two different theoretical interpretations for the low-energy structure of the lighter Po nuclei ($A \leqslant 200$), more detailed data on the positive parity states were needed. However, it is clear that the $^{200}$Po and $^{202}$Po nuclei play a key role in the discussion since the interpretation in the framework of the PCM model [9] is satisfactory for the heavier Po isotopes ($A>202$) while for the lighter Po isotopes two distinct descriptions are suggested. Therefore we examine the properties of the nonyrast $2_2^+$ and $4_2^+$ states of these two nuclei more carefully.

### D. Properties of the nonyrast states in $^{202,200}$Po

In $^{202}$Po, the $2_2^+$ state decays only to the $2_1^+$ state via a 79% $E2$/21% $M1$ transition (the ground-state transition was not observed; $I_\gamma < 0.3\%$). This is similar to the heavier Po isotopes but in contrast to the decay of the $2_2^+$ state in $^{200}$Po. This $2_2^+$ state decays via an $E2/M1/E0$ transition to the $2_1^+$ state and via a $\gamma$-ray transition of 1392.3 keV to the ground state. An indication for similar $E0$ strengths in $^{196}$Po and $^{198}$Po exists from in-beam measurements [8]. However a more recent in-beam experiment [10] did not provide evidence for missing $\gamma$-ray intensity due to an $E0$ component. This leaves the question about an important $E0$ component in the $2_2^+ \to 2_1^+$ transition for $^{196,198}$Po open but, out of the energy systematics as given in Fig. 9, the structure of this $2_2^+$ state in the lighter ($A \leqslant 200$) differs from the heavier isotopes ($A \geqslant 202$). An interpretation of the $2_2^+$ state in $^{200}$Po as member of a vibrational two-phonon multiplet is doubtful because of the $\Delta N_{\mathrm{ph}} = \pm 2$ selection rule for $E0$ transitions and the $\Delta N_{\mathrm{ph}} = \pm 1$ selection rule for $E2$ transitions. Instead the $E0$ component in the $2_2^+ \to 2_1^+$ transition in $^{200}$Po is compatible with the occurrence of an intruder configuration and thus of shape coexistence in this nucleus. When the two $2^+$ states have a different deformation and are mixed, strong $E0$ transitions can indeed be observed as was the case in the Pb isotopes [1,27]. Additional support for this interpretation is the ratio $X_{211} = B(E0;0_2^+ \to 0_1^+)/B(E2;0_2^+ \to 2_1^+)$. These ratios are presented in Table III for the four $0_2^+$ states that have been observed. The decrease of the $X_{211}$ values when going from, e.g., $^{200}$Po to $^{198}$Po, can again be explained by an increased mixing of the $2^+$ states. This increased mixing corresponds to an increased contribution of the deformed component in the $2_1^+$ wave function. The decay of the deformed $0_2^+$ state goes much faster towards the deformed component of the $2_1^+$ wave function than to the normal component. When reducing neutron number (and thus approaching midshell) the $2_2^+$ state decreases in energy due to the parabolic behavior of the $0_2^+$ bandhead energy and a considerable increase in mixing with the $2_1^+$ will result [7,26]. So an increased mixing of these $2^+$ states will give rise to an increase in the $B(E2;0_2^+ \to 2_1^+)$ values. The arguments given above to interpret the decrease of the $X_{211}$ values as due to an increased mixing between the $2^+$ states are depending on the fact that the $B(E0)$ value is not changing dramatically. This is indeed expected for the polonium nuclei with masses between 202 and 198. As calculated in Ref. [7] the contribution of the intruder configuration in the Po ground state is for these nuclei below the 10% level. From $^{196}$Po on, this mixing starts to become important, growing from 11% in $^{196}$Po to 58% in $^{192}$Po and thus the $X_{211}$ values will depend on a delicate ratio of mixing between all involved states.

TABLE III. Relative intensity branches for known $0_2^+$ states in Po.

| | $X_{211} = \dfrac{B(E0;0_2^+ \to 0_1^+)}{B(E2;0_2^+ \to 2_1^+)}$ |
|---|---|
| $^{202}$Po | $>8.3\times10^{-2}$ |
| $^{200}$Po | $>1.2\times10^{-2}$ |
| $^{198}$Po | $=5(3)\times10^{-3}$ |
| $^{196}$Po | $>10^{-3}$ |

Finally, it should be noted that in a recent $\alpha$-decay experiment of $^{192}$Po, evidence was found for considerable mixing of the $\pi$(4p-2h) intruder band head with the ground state of $^{192}$Po by its $\alpha$ decay [28]. When the difference in tunneling probability due to the difference in $\alpha$-particle energy is taken into account, the $\alpha$ decay of the $^{192}$Po $0^+$ ground state preferentially decays to the intruder state in $^{188}$Pb rather than to the Pb ground state, indicating that the ground state of $^{192}$Po is predominantly of $\pi$(4p-2h) character.

## V. CONCLUSION

We have presented a detailed level scheme of $^{202,200}$Po resulting from the $\beta$-decay and electron-capture study of $^{202,200}$At at LISOL. These nuclei were expected to be very similar to the heavier Po isotopes. We showed that due to the special deexcitation pattern of the nonyrast $0_2^+$ and $2_2^+$ states, $^{202}$Po and $^{200}$Po cover a transition region between the heavier Po isotopes where the positive parity states can be explained as members of pure two-phonon multiplets in a quadrupole vibrational model and $^{200}$Po where a $\pi$(4p-2h) deformed band intrudes into the low-energy part of the excitation spectrum and mixes with the ground state. This enforces the interpretation of low-lying intruder $0^+$ states in the lighter Po isotopes, but for the interpretation of the $I \neq 0$ states, more experimental data (conversion coefficients, transition rates, etc.) as well as theoretical studies in a PCM or intruder framework are needed to exclude one or the other.

## ACKNOWLEDGMENTS

We would like to thank J. Gentens and P. Van Den Bergh for running and maintaining the LISOL separator. M.H., G.V., and S.F. would like to thank the FWO Belgium for financial support.


[1] J. L. Wood, K. Heyde, W. Nazarewicz, M. Huyse, and P. Van Duppen, Phys. Rep. **215**, 101 (1992).

[2] K. Heyde, J. Jolie, J. Moreau, J. Ryckebusch, M. Waroquier, P. Van Duppen, M. Huyse, J. L. Wood, Nucl. Phys. **A466**, 189 (1987).

[3] E. Coenen, K. Deneffe, M. Huyse, P. Van Duppen, and J. L. Wood, Phys. Rev. Lett. **54**, 1783 (1985).

[4] M. Huyse, E. Coenen, K. Deneffe, P. Van Duppen, K. Heyde, and J. Van Maldeghem, Phys. Lett. B **201**, 293 (1988).

[5] J. Wauters, P. Dendooven, M. Huyse, G. Reusen, P. Lievens, P. Van Duppen, and the ISOLDE Collaboration, Z. Phys. A **344**, 29 (1992).

[6] J. Wauters, N. Bijnens, P. Dendooven, M. Huyse, H-Y. Hwang, G. Reusen, J. von Schwarzenberg, P. Van Duppen, R. Kirchner, E. Roeckl, and the ISOLDE Collaboration, Phys. Rev. Lett. **72**, 1329 (1994).

[7] N. Bijnens *et al.*, Phys. Rev. Lett. **75**, 4571 (1995).

[8] D. Alber *et al.*, Z. Phys. A **339**, 225 (1991).

[9] W. Younes and J. A. Cizewski, Phys. Rev. C **55**, 1218 (1997).

[10] L. A. Bernstein *et al.*, Phys. Rev. C **52**, 621 (1995).

[11] W. Younes *et al.*, Phys. Rev. C **52**, R1723 (1995).

[12] K. Helariutta *et al.*, Phys. Rev. C **54**, R2799 (1996).

[13] N. Fotiades *et al.*, Phys. Rev. C **55**, 1724 (1997).

[14] M. Huyse, P. Decrock, P. Dendooven, J. Gentens, G. Vancraeynest, P. Vandenbergh, and P. Van Duppen, Nucl. Instrum. Methods Phys. Res. B **70**, 50 (1992).

[15] R. Kirchner, K. H. Burkhard, W. Hl̈ler, and O. Klepper, Nucl. Instrum. Methods Phys. Res. **186**, 295 (1981).

[16] H. Beuscher, D. R. Zolnowski, D. R. Haenni, and T. T. Sugihara, Phys. Rev. Lett. **36**, 1128 (1976).

[17] B. Fant, T. Weckström, and A. Källberg, Phys. Scr. **41**, 652 (1990).

[18] M. Huyse, P. Decrock, P. Dendooven, G. Reusen, P. Van Duppen, and J. Wauters, Phys. Rev. C **46**, 1209 (1992).

[19] X. Rösel, H. M. Fries, K. Alder, and H. C. Pauli, At. Data Nucl. Data Tables **21**, 381 (1978).

[20] A. Maj, H. Grawe, H. Kluge, A. Kuhnert, K. H. Maier, J. Recht, N. Roy, H. Hübel, and M. Guttormsen, Nucl. Phys. **A509**, 413 (1990).

[21] R. B. Firestone, *Table of Isotopes* (John Wiley & Sons, New York, 1996).

[22] V. Rahkonen, B. Fant, and C. J. Herrlander, Phys. Scr. **34**, 720 (1986).

[23] A. Maj, H. Grawe, H. Kluge, A. Kuhnert, K. H. Maier, R. A. Meyer, J. Recht, and N. Roy, Z. Phys. A **324**, 123 (1986).

[24] P. J. Brussaard and P. W. M. Glaudemans, *Shell-Model Applications in Nuclear Spectroscopy* (North-Holland, Amsterdam, 1977).

[25] I. Bergström, J. Blomqvist, C. J. Herrlander, J. Hattula, O. Knuuttila, E. Liukkonen, and V. Rahkonen, Z. Phys. A **287**, 219 (1978).

[26] N. Bijnens, Dissertation, Leuven, 1998, unpublished.

[27] K. Heyde and R. A. Meyer, Phys. Rev. C **37**, 2170 (1988).

[28] N. Bijnens *et al.*, Z. Phys. A **356**, 3 (1996).